Progress in Natural Science: Materials International (xxxx) xxxx–xxxx

HOSTED BY

ELSEVIER

Contents lists available at ScienceDirect

Progress in Natural Science: Materials International

journal homepage: www.elsevier.com/locate/pnsmi

Review

Recent advances in additive-enhanced magnesium hydride for hydrogen storage☆

Ying Wang[a,b], Yijing Wang[b,c,*]

[a] School of Chemistry and Chemical Engineering, Jiangsu Key Laboratory of Green Synthetic Chemistry for Functional Materials, Jiangsu Normal University, Xuzhou, Jiangsu 221116, China

[b] Key Laboratory of Advanced Energy Materials Chemistry, Nankai University, Tianjin 300071, China

[c] Collaborative Innovation Centre of Chemical Science and Engineering (Tianjin), Nankai University, Tianjin 300071, China

ARTICLE INFO

Keywords:
Hydrogen storage
MgH_2
Additives
Alloying
Nanoscaling
Nanoconfinement

ABSTRACT

The discovery of new hydrogen storage materials has greatly driven the entire hydrogen storage technology forward in the past decades. Magnesium hydride, which has a high hydrogen capacity and low cost, has been considered as one of the most promising candidates for hydrogen storage. Unfortunately, extensive efforts are still needed to better improve its hydrogen storage performance, since MgH_2 suffers from high operation temperature, poor dehydrogenation kinetic, and unsatisfactory thermal management. In this paper, we present an overview of recent progress in improving the hydrogenation/de-hydrogenation performance of MgH_2, with special emphases on the additive-enhanced MgH_2 composites. Other widely used strategies (e. g. alloying, nanoscaling, nanoconfinement) in tuning the kinetics and thermodynamics of MgH_2 are also presented. A realistic perspective regarding to the challenges and opportunities for further researches in MgH_2 is proposed.

1. Introduction

What hampers our step towards a hydrogen-based energy system? Although plenty of issues, such as hydrogen generation, hydrogen transportation, hydrogen application, must be solved in our way to fulfil the worldwide commercial usage of hydrogen, it is the lack of ideal hydrogen storage material that primarily blocks the progress of hydrogen technology. The discovery of each novel hydrogen storage material (alloys, carbon materials, metal organic frameworks (MOFs), organic liquids, metal alanates, metal hydrides et al. [1–7]) had greatly promoted the revolution of hydrogen storage technology.

An ideal hydrogen storage material should meet the following standards: (1) cost-affordable, (2) high hydrogen storage capacity (5.5 wt% and 40 g L^{-1} hydrogen capacity by 2020, U.S. Department of Energy [8]), (3) mild operation temperature and easy to absorb/de-absorb hydrogen, (4) long life-span. Fig. 1 showed some typical hydrogen storage technologies and compared their operation conditions [9]. Apparently, amongst all these strategies, metal hydrides exhibit huge potential for commercial storage of hydrogen. Especially, MgH_2 has been considered as one of the most promising candidates, due to its high hydrogen storage capacity (7.6 wt%, 110 g L^{-1} H_2), abundance in deposit, and low cost.

MgH_2 is an ionic compound and its charge distribution is $Mg^{1.91+}H^{0.26-}$. This structure results a high thermodynamic stability of MgH_2, which shows an enthalpy value of 74.7 kJ mol^{-1}, and an entropy value of 130 J K^{-1} mol^{-1}. The high stability of MgH_2 leading to a high operation temperature (> 350 °C) which is not good for practical application. Another drawback of MgH_2 is its sluggish sorption kinetics, causing by the following reasons: (1) existence of oxide on its surface, (2) slow diffusion rate of hydrogen in the bulk MgH_2/Mg, (3) poor decomposition of hydrogen on the Mg surface [10]. Additionally, the unsatisfactory heat management of MgH_2/Mg also affects its hydrogenation/de-hydrogenation behaviours. All these problems above have hampered the worldwide application of MgH_2/Mg. To date, numerous efforts have been carried out to overcome these disadvantages, and huge improvements have been achieved. For example, Xia et al. synthesized monodisperse MgH_2 nanoparticles (NPs) that anchored on graphene sheet, and confirmed its impressive hydrogen storage properties, which released 5.4 wt% hydrogen within 30 min and showed an ultra-long cycle-life of 100 times [11].

In this paper, we summarized a wide range of promising strategies to tuning the hydrogen storage performance of MgH_2/Mg, with special focus on the advantages and challenges of each method. To better present the research progress of MgH_2/Mg, we classified the technologies into four categories: alloying, nanoscaling, nanoconfinement, and additive-addition. Rather than detail all outcomes of each classic

Peer review under responsibility of Chinese Materials Research Society.

* Corresponding author.
E-mail address: wangyj@nankai.edu.cn (Y. Wang).

http://dx.doi.org/10.1016/j.pnsc.2016.12.016
Received 28 October 2016; Accepted 30 November 2016
1002-0071/

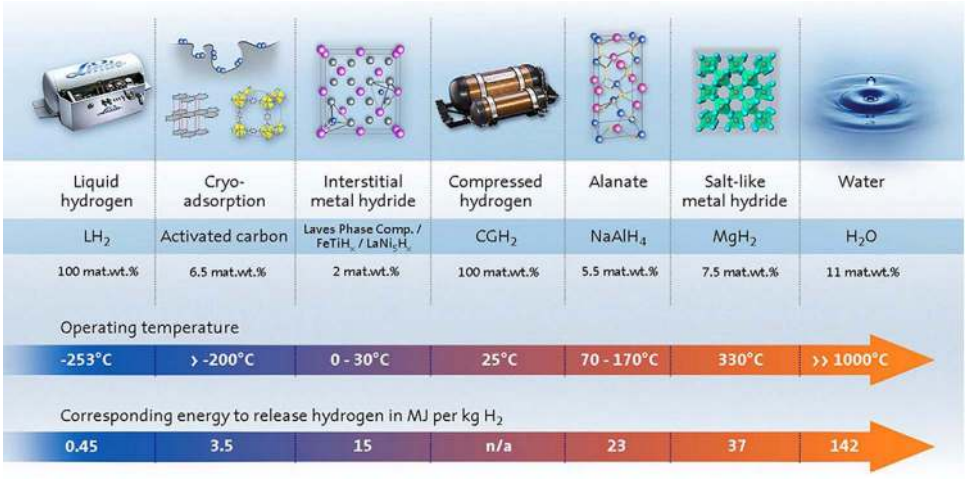

Fig. 1. Comparison of different hydrogen storage strategies and their operation conditions [8].

method, we pay especial attention on the additive-enhanced MgH_2 systems. By reviewing these data, we hope this paper can help more researchers better understanding MgH_2, and shed light on further works.

2. Overview of tuning strategies

The hydrogenation/de-hydrogenation process of MgH_2/Mg is illustrated in Fig. 2. Apparently, decreasing the energy barrier and/or changing the reaction enthalpy of MgH_2/Mg are fundamental ways to improve its hydrogen storage performance.

2.1. Alloying

One of the most effective methods to reduce the thermodynamic barrier of MgH_2/Mg is alloying. Instead of direct reaction between MgH_2 and Mg, the formation of Mg-alloys changes its sorption path. By forming thermodynamic more stable alloys, the operation temperature of MgH_2/Mg can be reduced. Various elements had been used to alloy with Mg, including rare earth elements, transition metals, and partial main group elements [12–24]. Table 1 summarizes the basic properties of some commonly investigated Mg-based hydrogen storage alloys.

Mg_2NiH_4, which has a lower enthalpy of 64 kJ mol^{-1}, is one of the most investigated Mg-alloys [37–39]. Kumar et al. reported that the hydrogen sorption of nanocrystalline Mg_2NiH_4 alloy started at 200 °C. However, the Mg_2NiH_4 alloys exhibited a low hydrogen capacity of only 3.6 wt%. Meanwhile, Mg_2FeH_6, which has a higher theoretical hydrogen capacity of 5.5 wt%, shows an even high enthalpy of 95 kJ mol^{-1} H_2[40–43]. Chen et al. reported the hydrogen storage performance of

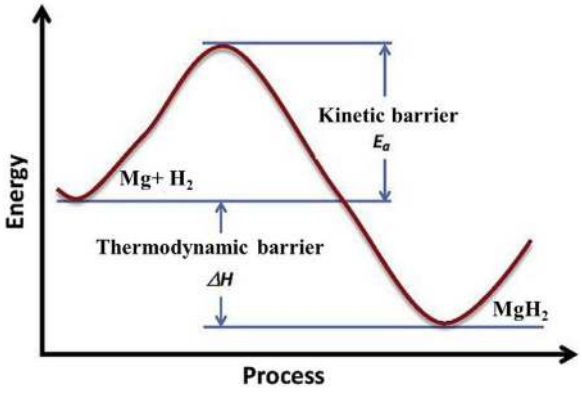

Fig. 2. Illustration for the hydrogenation/de-hydrogenation process of MgH_2/Mg.

Table 1
Fundamental information of some Mg-based alloys [25].

Name	E_a (kJ mol^{-1})	ΔH (kJ $mol^{-1}H_2$)	Capacity (wt%)	T (°C)	Ref.
Mg	–	74.5	7.6	300	Stampfer [26]
Mg (2–7 nm)	–	71.2	7.6	276	Paskevicius [27]
$Mg_{90}Ce_{10}Ni_{10}$	109.2	77.9	5.4	284	Lin et al.[28]
Mg_2Ni	–	64.5	3.6	254	Reilly [29]
$Mg_3LaNi_{0.1}$	–	81	2.73	284	Ouyang [30]
Mg_3Cd	69	65.5	2.8	–	Skripnyuk.[31]
MgH_2-Ti	30.8	75.2	6.7	278	Cui [32]
$Mg_{0.95}In_{0.05}$	–	68.1	5.3	–	Zhong [33]
Mg_3Ag	–	68.2	2.1	–	Si [34]
Mg_2Si	–	36.4	5.0	–	Vajo [35]
Mg_5Ga_2	149	68.7	5.7	300	Ouyang [36]

Mg_2FeH_6@MgH_2 core-shell, which released 5.0 wt% hydrogen within 50 min at 280 °C [14]. In 2012, Liu et al. reported the hydrogen storage properties of Mg@$Mg_{17}Al_{12}$ particles, which delivered 6.0 wt% hydrogen with 30 min at 350 °C, and absorbed 7.0 wt% hydrogen at 400 °C [44]. As shown in Fig. 3, the $Mg_{17}Al_{12}$ shell enclosed Mg core and effectively resisted the formation of MgO. The shell grown with the increased content of Al, but over high Al content would broke this core-shell structure.

Fig. 4 showed the de-hydrogenation/hydrogenation performance of $LaMg_{11}Ni$+x wt% Ni alloys [15]. Zhang et al. found that milling time and Ni content were both essential factors for enhancing the kinetics of $LaMg_{11}Ni$+x wt% Ni alloys. Good improvement was achieved for the $LaMg_{11}Ni$+200 wt% Ni sample, which absorbed 6.41 wt% hydrogen within 18 min, and reduced E_a to only 68.5 kJ mol^{-1}. Additionally, the $Mg_{6-7}TMH_{12-16}$ (TM=Ti, Zr, Hf, V, Nb), which have a similar structure with CaF_2, also gained huge attention. The $Mg_{6-7}TiH_{12-16}$ releases 4.7 wt% hydrogen at 330 °C, but its re-hydrogenation process is rather tough.

Generally, Mg-base hydrogen storage alloys can effective decrease the operation temperature, but the introduction of heavy metals also result a decreased hydrogen capacity in the system, and most of these Mg-base alloys still suffered from poor reversibility. Detail information about these Mg-based hydrogen storage alloys can refer to a recent review [24].

2.2. Nanoscaling

Nanoscaling has proven its possibility in optimizing the thermodynamics and kinetics of MgH_2. Theoretical calculation (based on the first principle theory) has predict that when reducing the grain size of

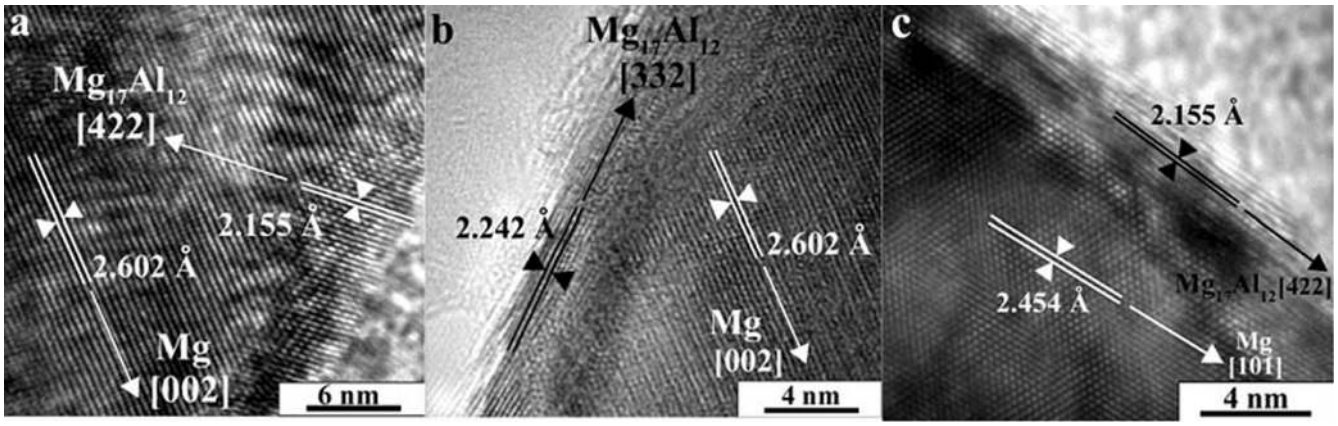

Fig. 3. HR-TEM images of (a) Mg-7 at%Al, (b) Mg-22 at% al, (c) Mg-27 at% Al [44].

MgH_2 to < 3 nm, both its thermodynamic and kinetics can be greatly improved [45]. And kinetics improvement still exists when the particle size of MgH_2 is below 50 nm. These enhancements of nanoscaling can be assigned to the following reasons: (1) increased fresh surface, (2) decreased diffusion distance for hydrogen, (3) intimate contract between reactants, (4) condensed atoms in the grain boundaries. To date, plenty of works have done to prepare MgH_2 NPs including: ball-milling, hybrid combustion, melt spinning, and chemical vapour deposition (CVD) [46–53].

Chen et al. found that MgH_2 nanowires had a lower dehydrogenation energy barrier (33.5 and 38.8 kJ mol^{-1} for hydriding and dehydriding) than that of bulk MgH_2 (120–142 kJ mol^{-1}), predicting that decreasing the nanowires to thinner than 30 nm could change both the thermodynamics and kinetics of MgH_2 [54]. By comparing the hydrogen storage properties of different size MgH_2 (25, 32, and 38 nm), Prieto et al. confirmed that the hydrogen sorption kinetics were faster when the particle size smaller [55]. The 25 nm MgH_2 absorbed 95% hydrogen within 60 s at 300 °C, and show a lowest E_a value of only 122 kJ mol^{-1}. Ouyang et al. found that reducing the Mg/Mg_2Ni NPs to 20 nm its hydrogen storage performance would greatly improve [56]. As shown in Fig. 5, different shapes MgH_2/Mg NPs can be prepared *via* control the deposition temperature, hydrogen pressure, and time during the hydriding CVD process, this work demonstrated the possibility of produce on-demand MgH_2 particles for hydrogen storage [57]. In 2012, Akiyama further studied the hydrogen sorption performance of zebra-striped MgH_2 fibres [58]. Fig. 6 compared the isothermal sorption curves of this MgH_2 fiber with commercial MgH_2 powder. The fibered MgH_2 exhibited best hydrogen storage perfor-

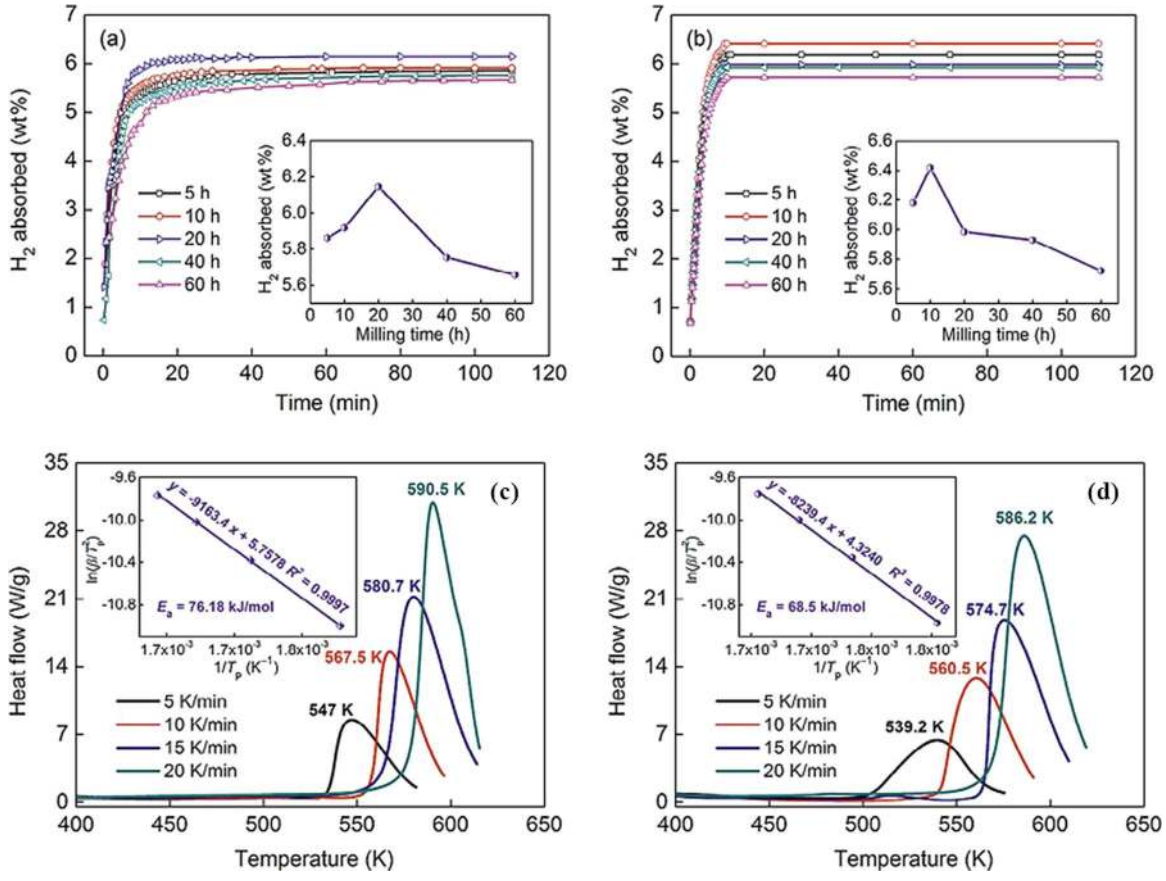

Fig. 4. Hydrogen absorption curves of $LaMg_{11}Ni$+x wt% Ni (x=100, 200) alloys at 593 K, (a) x=100, (b) x=200. DSC curves and Kissinger plots of $LaMg_{11}Ni$+x wt% Ni (x=100, 200) alloys (c) x=100, and (d) x=200 [15].

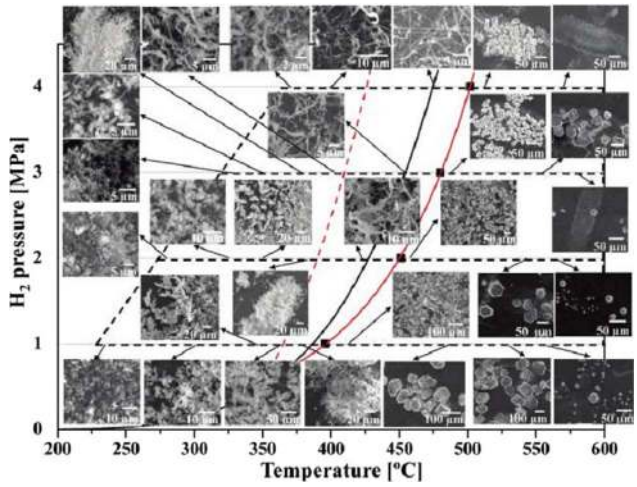

Fig. 5. Morphologies of MgH_2 samples, under different preparation conditions [57].

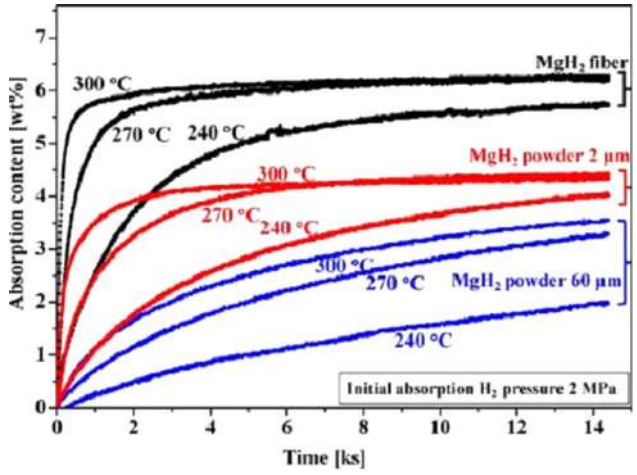

Fig. 6. Isothermal hydrogen absorption curves of different MgH_2 sample [58].

mance with 6.0 wt% hydrogen desorbed in 3000 s, and > 75% hydrogen absorbed within 200 s.

Although nanoscaling greatly benefits the hydriding/de-hydriding of MgH_2/Mg, the high surface energy of NPs may result serious aggregation during cycling, and sluggishly decreasing the advantages of those nanocrystallization. Therefore, finding a proper method to protect the NPs from aggregation is highly needed.

2.3. Nanoconfinement

To keep MgH_2/Mg in nanoscale, nanoconfinement is proposed, which embedding the MgH_2/Mg NPs into a stable scaffold and therefore hinders the particle growth and agglomeration. By tuning the pore diameter of scaffold, MgH_2/Mg with various sizes can be obtained. Basic requirements for the scaffold materials are as following: (1) chemical inertness, do not react with any reactants; (2) structural stable during the continuous hydriding/de-hydriding; (3) high surface area to tolerate more active materials; (4) high volume ratio and uniform pore size distributions. The most used scaffolds are porous carbons, metal-organic frameworks, porous polymer et al.. Table 2 showed an overview of some wildly used scaffolds to confine the MgH_2/Mg NPs.

Jongh et al. obtained 6, 9, 12, 20 nm MgH_2 NPs by using CA (pore size 6–20 nm) as scaffold [67]. Investigations confirmed that the MgH_2 particle size was correlated to the pore size of the scaffolds, and the existence of CA effectively hampered the particle grow and aggregation of MgH_2/Mg during the cycling [67]. In 2015, Yu et al. reported simple

Table 2
Summary of some wildly used scaffolds and their loading content.

Sample	Pore size (nm)	Precursor	Solvent/ Atmosphere	Loading (wt %)	Ref.
RF-CA[a]/MgH_2	22	$MgBu_2$	Heptane/Ar	18.2	[59]
RF-CA/MgH_2	7	$MgBu_2$	Heptane/Ar	10.0	[59]
RF-CA/MgH_2	13	$MgBu_2$	Ar	14.8	[60]
AC(fiber)[b]/ MgH_2	0.5–3	$MgBu_2$	Ar	22.0	[61]
RF-CA(Ni)/ MgH_2	13	MgH_2	Ar	9.6	[62]
RF-CA(Cu)/ MgH_2	13	MgH_2	Ar	12.7	[62]
RF-CA/MgH_2	13	MgH_2	Ar	3.6	[62]
HSAG[c]/MgH_2	2–3	MgH_2	Ar	10–15	[63]
AC[d]/MgH_2	< 2	MgH_2	Ar	15–20	[63]
CA/MgH_2	6–20	MgH_2	Ar	10	[64]
CMK–3/MgH_2	3.9	$MgBu_2$	Heptane/Ar	20	[65]
SBA–15/MgH_2	5–10	$MgBu_2$	Heptane/Ar	17	[66]

[a] Resorcinol–formaldehyde carbon aerogels.
[b] Carbon aerogels.
[c] High surface area graphite.
[d] Activated carbon.

method to synthesis monodispersed MgH_2 NPs that self-assembled on graphene sheet (MHGH, Fig. 7) [11]. Further doped the MHGH with Ni, the resultant Ni-MHGH sample demonstrated even better hydrogen storage performance, with ultra-long cycling life and fast desorption/sorption kinetics.

Basic reasons for these improved hydrogen storage performance caused by nanoconfinement can be ascribed as following: enlarged contact surface of reactants, increased grain boundaries, decreased H diffusion distance, and good resistance of the particle growth and agglomeration. The outcomes of nanoconfinement swingeing promoted the cycle stability of MgH_2, however, drawbacks still exist. The hydrogen capacity of nanoconfined MgH_2 system is decreased due to its limited loading amount. The kinetics is relatively slow compared with the catalyzed MgH_2. Further design and synthesize multifunctional scaffolds with high surface area and specific catalysts is needed.

3. Additive-enhanced MgH_2/Mg composites

3.1. Adding catalysts

Generally, adding catalysts is one of the most effective and easy-to-handle ways to enhance the hydrogen storage performance of MgH_2/Mg. Numerous catalysts (carbons, metals, metal oxides, metal halides, and covalent compounds et al.) had been introduced into MgH_2 system and great improvements were reported. Table 3 overviews some generally used catalysts in MgH_2.

According to the hydrogen spillover mechanism, the catalysts perform better with porous structure and high surface area, which favour the hydrogen dissociation [45,89,90]. In spillover, the hydrogen dissociates on the catalyst, while some hydrogen atoms still attach to the catalyst, other atoms diffuse to the support, slowly penetrate into the metal, and interact with the metal. With the help of a proper catalyst this process can diffuse through the MgO layers. For example, Hudson et al. found that the G-Fe (Fe NPs anchored on graphene) not only improved the dehydrogenation behaviour of MgH_2, but also enhanced the hydrogenation of Mg to MgH_2 through the spillover effect [91]. The MgH_2-G-Fe system released hydrogen at 281 °C and showed a lower energy barrier of 119 kJ mol^{-1}.

Except of surface catalyst, kinetics enhancement of MgH_2 also observed by doping catalyst inside its particles. Zhu et al. reported that the multi-valence Ti coated MgH_2 system (Mg-Ti) started to desorb hydrogen at 175 °C and 5 wt% hydrogen was released within 15 min at 250 °C [32]. Thermodynamic property of this Mg-Ti was changed to a

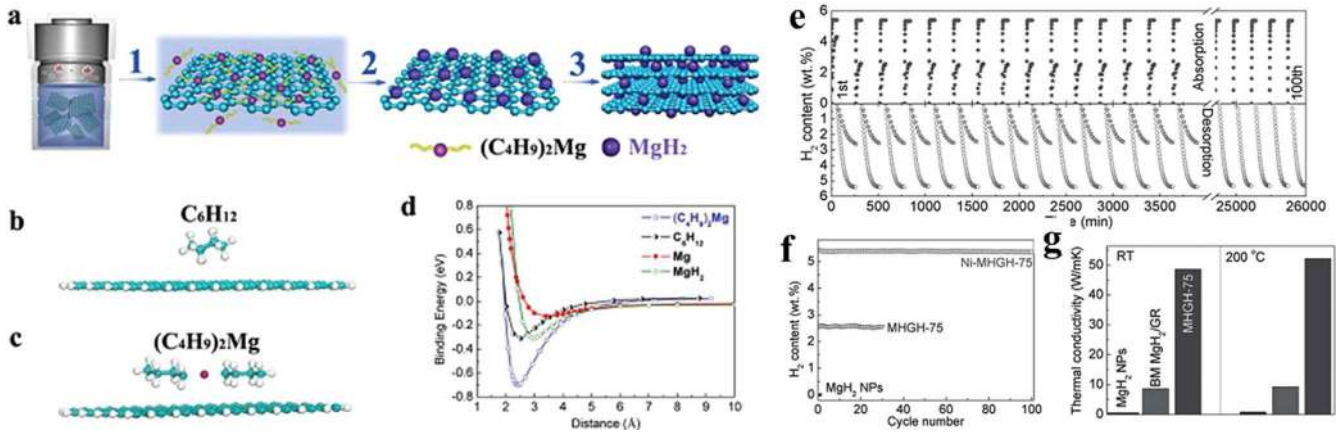

Fig. 7. (a) Schematic illustration of the self-assembling MgH_2 NPs on GR, (b) C_6H_{12} and (c) $(C_4H_9)_2Mg$ on a GR sheet under the most stable configuration, (d) binding energy curves based on density functional theory (DFT) calculations. (e) Reversible H_2 sorption, (f) cycling of Ni-MHGH-75, MHGH-75, and MgH_2 NPs at 200 °C. (g) thermal conductivity of MHGH-75 [11].

more favourable state. Fig. 8 demonstrated the possible mechanism for these improvements. For the MgH_2–5% Nb system, Pelletier et al. confirmed that the Nb acted as gateway for the hydrogen leaving [73]. Barkordarian et al. carried out another study on the MgH_2-Nb_2O_5 system [92]. And reported the fastest absorption accrued in the MgH_2–0.5 mol% Nb_2O_5, and the absorption kinetics was related to the concentration of Nb_2O_5. Our group systematically investigated the effects of different Ti-based materials on dehydrogenation performance of MgH_2, and the results indicated that even the catalysts all contained Ti element, TiN, TiO_2, TiF_3, and Ti showed their catalytic effect through different ways [46]. A series of combined catalysts also added into MgH_2, i. e. Ni/Al_2O_3/C [93], SiC/Ni [86], TiH_2/Mg_2Ni [94], Fe/Ti [95].

Besides all the metal-based catalysts above, carbon-based materials also show huge potential in improving the hydrogen storage performance of MgH_2. Plenty of works devoted to combine MgH_2 with various carbon materials, including but not limited to carbon nanotubes (CNTs), C_{60}, carbon nanofibers (CNFs), graphite, AC [97–99]. Previously, our group investigated the catalytic effects of graphene nanosheets (GNS) on hydrogenation/de-hydrogenation of MgH_2. As shown in Fig. 9, extending the ball-milling time made the MgH_2–5 wt% GNS decreased in its grain size and hydrogenation peak temperature [96]. Mechanism investigation found that the GNS served as both

Table 3
Summery of some widely used catalysts in MgH_2.

Catalyst	Method	Amount	Phenomenon	Ref.
B	BM 59 h	Mg–2B	Significant oxide observed	Varin [43]
Co	RBM 0.5–10 h	10, 20 wt%	Crystallite and particle sizes	Bobet [68]
Cu	SFCD	0.4, 1 wt%	Good kinetic under high T	Denis [69]
Fe	BM20h	5 wt%	Thermodynamics unchanged	Liang [70]
Ge	RBM	5 at%	Mg_2Ge formed	Gennari [71]
Gd	Ar arc	5 wt%	Gd_2O_3 observed	Zou [72]
Mn	BM 20 h	5 at%	Thermodynamics unchanged	Liang [70]
Nb	BM 20 h	5 at%	Unstable NbH_x found	Pelletier [73]
Nd	Ar Arc	5 wt%	Nd_2O_3 found	Zou et al.[72]
Pd	RBM 0–20 h	1 wt%	Enhanced due to small size	Zaluski [74]
Pt	Wet chemi	0.5 mol.%	Spillover mechanism	Xu [75]
V	BM 2 h	5 wt%	No significant improvement	Gasan [76]
Al_2O_3	BM 100 h	1 mol.%	0.2 mol% sufficient catalyst	Oelerich [77]
CeO_2	RBM 2 h	10 wt%	20% conversion	Song [78]
Cr_2O_3	BM 100 h	0.2–5 mol.%	Cr_2O_3 reduced gradually	Song [78]
CuO	BM 100 h	5 mol.%	0.2 mol% sufficient catalyst	Oelerich [77]
Fe_2O_3	BM 20 h	1.5–2.5 wt%	Enthalpies not changed	Polanski [79]
Fe_3O_4	BM 100 h	5 mol.%	Destabilized phase found	Borgschulte [77]
In_2O_3	BM 20 h	3–4 wt%	Enthalpies not changed	Polanski [79]
Mn_2O_3	BM 100 h	5 mol.%	0.2 mol% sufficient catalyst	Oelerich [79]
Nb_2O_5	BM 20 h	1 mol.%	Nb_2O_5 reduced	Hanada [80]
SiO_2	BM 100 h	5 mol.%	0.2 mol% sufficient catalyst	Oelerich [77]
TiO_2	RBM0.5–5 h	20 wt%	γ-MgH_2 after 4 h	Wang [81]
ZnO	BM 20 h	6.5–10 wt%	Enthalpies not changed	Polanski [82]
VO_2	BM 10 h	10 wt%	Decrease in crystallite size	Milosevic [83]
$CrCl_3$	BM 12 h	5 wt%	Mg surface modification	Ivanov [84]
CeF_2	BM 15 min	1–10 mol.%	Little effect	Jin [85]
CuF_2	BM 15 min	1–10 mol.%	Cu_2Mg formed	Jin [85]
TiF_3	BM 15 min	1–10 mol.%	TiH_2 formed	Jin [85]
NbF_5	BM 15 min	1–10 mol.%	NbH formed	Jin [85]
VF_4	BM 15 min	1–10 mol%	V_3H_2 formed	Jin [85]
SiC	BM 24 h	5 wt%	Increase surface area and defects	Ranjbar [86]
TiC	BM 30 min	2 at%	Enhanced kinetics	Pitt [87]
VN	BM 100 h	5 mol%	V compound better than V	Oelerich [88]

BM: ball-milling, RBM: random ball-milling, SFCD: supercritical fluid chemical deposition, Wet chemi: wet chemistry.

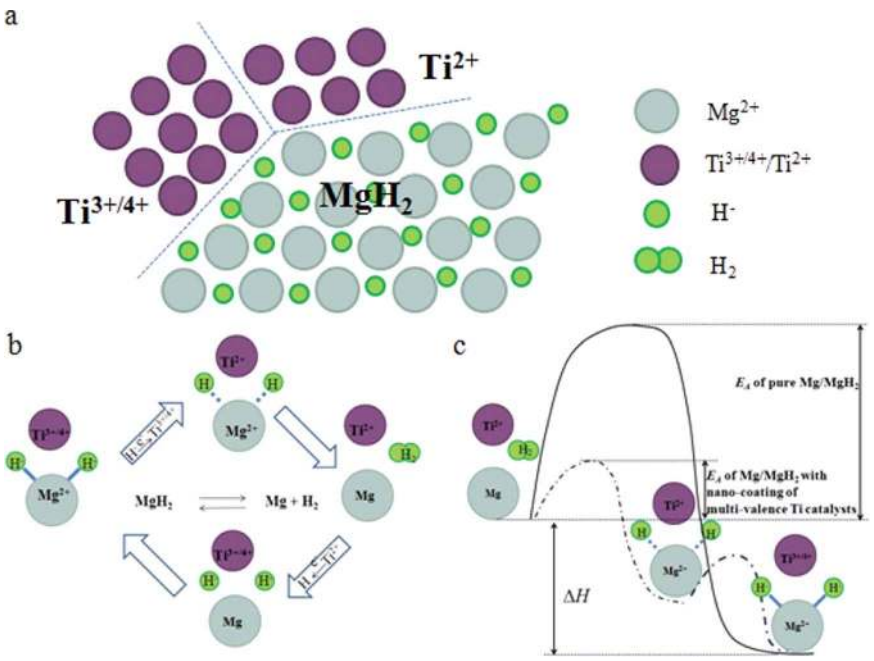

Fig. 8. Schematic for the catalytic mechanism of muti- valence Ti doped MgH_2[32].

dispersion matrix and catalysts for hydrogen diffusion. CNTs and CNFs were found to show better catalytic effects than their competitors. It suggested that the added carbon nanotubes acted as channels for faster hydrogen diffusion, and the metal impurities in CNTs and CNFs also promoted the hydrogenation/de-hydrogenation process. In general, all carbon materials show positive effects on MgH_2 (improving kinetics and cycle-life), however, no thermodynamic changes of MgH_2 were reported when using carbons as additives [46].

Hybrids of metal-based materials and carbons are new catalogue of promising additive for tuning the hydrogen storage performance of MgH_2. With the benefits of both carbon and metal-based catalyst, these hybrids show some amazing features: (1) high surface area, which is favourable for intimate contact between MgH_2 and catalyst, (2) high activity, combining metal elements with carbon shows the possibility to tuning both thermodynamic and kinetic properties of MgH_2, (3) extended life-span, the presence of carbon well maintained the structural stability of catalyst and resulted continuous improvement in MgH_2. In fact, plenty of works have proven the superior catalytic effects of these hybrids on MgH_2.

Our group first reported the synthesis of TiN@rGO hybrid (Fig. 10), and studied its enhanced catalytic effects on the dehydrogenation performance of MgH_2, which outperformed individual TiN and rGO. The as-obtained TiN@rGO showed a high surface area (177 $m_2\ g^{-1}$) and more defects, which greatly promoted the dehydriding of MgH_2. The MgH_2-TiN@rGO released hydrogen at 167 °C, and 6.0 wt% hydrogen released within 18 min at 300 °C. Similar improvements were observed in the MgH_2-TiB_2/GNS composites, which confirmed the synergistic effect between GNS and TiB_2[100]. Zhuet al. carried out a further study on the effects of CNTs supported Ni on MgH_2[101]. An excellent hydrogen storage performance was revealed, the Mg85-(Ni/CNTs) composites absorbed 5.68 wt% hydrogen within 100 s at 100 °C, and released 4.31 wt% hydrogen within 1800 s at 250 °C. Other well studied metal/carbon hybrids are Ni/C, Co/C, NiCo/C et al. [48,102–104]. Fig. 11 compared the cycle stability of pure MgH_2 and MgH_2-NiCo/rGO sample, indicating the hydrogen capacity and enhanced kinetics of MgH_2 were well maintained with the help of NiCo/rGO.

Although lots of literatures had proven adding catalysts as the most useful method to improve the hydrogen storage performance of MgH_2, and enhancements were observed in all cases, specific mechanism behinds a certain MgH_2-catalyst system is still not fully understood. More attentions should be paid to understanding the reason behind.

3.2. Mixing with other metal hydrides

Combining with other light metal hydride paves a new way for MgH_2 to overcome its thermodynamic and kinetic drawbacks.

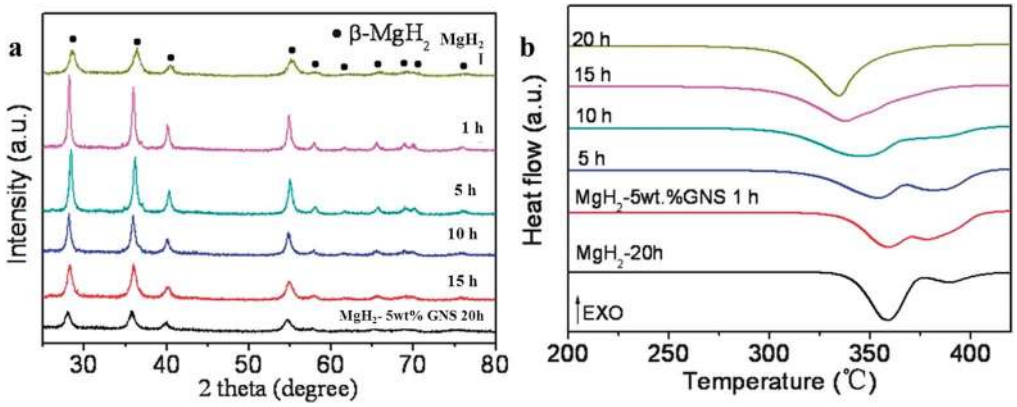

Fig. 9. (a) XRD plots, and (b) DSC curves for the MgH_2–5 wt% GNS system [96].

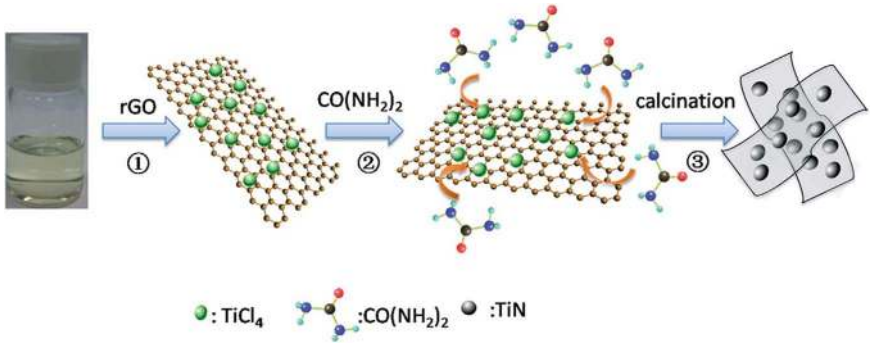

Fig. 10. Illustration for the preparation of TiN@rGO hybrid [47].

Basically, the added light metal hydride alters the dehydriding/hydriding pathway of MgH_2/Mg, and contributes hydrogen capacity to the new composite. Take MgH_2-$LiAlH_4$ for example, the dehydrogenation of pure $LiAlH_4$ occurs according to Equation 1–2. But when mixed with MgH_2, the dehydrogenation process of this new system happed according to Equation 1–4 [106]. Apparently, during the dehydriding, $LiAlH_4$ and MgH_2 interacts each other, and a thermodynamically more stable MgAl alloy formed which favours the process. Recently, Utkeet al. proposed that besides the superior dehydriding/hydriding performance the MgH_2-$NaAlH_4$ sample also demonstrated good reversibility [107]. The widely studied hydride composites including: MgH_2-$NaAlH_4$, MgH_2-AlH_3, MgH_2-$LiBH_4$-$NaAlH_4$, MgH_2-$LiNH_2$-$LiBH_4$, MgH_2-$LiBH_4$-Al et al. Table 4 lists the hydrogen storage performance of some MgH_2 composites.

$$3LiAlH_4 \rightarrow Li_3AlH_6 + 2Al + 3H_2 \quad (1)$$

$$Li_3AlH_6 \rightarrow 3LiH + Al + 3/2H_2 \quad (2)$$

$$4{\cdot}08MgH_2 + 0{\cdot}92LiH \rightarrow Li_{0.92}Mg_{4.08} + 4{\cdot}54H_2 \quad (3)$$

$$17MgH_2 + 12Al \rightarrow Al_{12}Mg_{17} + 17H_2 \quad (4)$$

Inspired by the significant hydrogen storage performance of these MgH_2-metal hydride composited, our group further studied the destabilization effects of $Mg(AlH_4)_2$ on MgH_2. The dehydrogenation performance of this MgH_2-$Mg(AlH_4)_2$ composite was shown in Fig. 12. The MgH_2-$Mg(AlH_4)_2$ started to release hydrogen at 90 °C and had a high hydrogen capacity of 7.6 wt%, which was outstanding among other composites. Mechanism investigations found that the destabilization effects of $Mg(AlH_4)_2$ on MgH_2 happened on both kinetics and thermodynamics' aspects. Further researches on reversibility of these MgH_2-metal hydrid should be performed.

Table 4
Hydrogen storage performance of MgH_2 combined with other hydride.

Sample	Amount	Method	Phenomenon	Ref.
AlH_3	50 mol.%	BM 0.5 h	$Mg_{17}Al_{12}$, Al_3Mg_2 seen	Liu [108]
$LiBH_4$	10 mol.%	BM 15 h	MgB_2 formed	Johson [109]
$NaBH_4$	10 wt%	BM 100 h	MgB_2 formed	Czujko [110]
$LiAlH_4$	20 mol.%	BM 1 h	Mg-Al alloys formed	Mustafa [106]
$NaAlH_4$-$LiBH_4$	66 mol.%	BM 1 h	Mg-Al alloys formed	Plerdsanoy [111]

4. Conclusion and perspectives

MgH_2, as one of the most promising hydrogen storage candidate, meet most criteria for practical application: high hydrogen capacity, low cost, high deposit, and non-toxic. The main drawbacks that hinder MgH_2 from commercial usage are its high stability, poor kinetics, and severe thermal management. So far, enormous efforts have been paid to overcome these disadvantages. In this review, we summary the most effective ways to altering the hydrogen storage performance of MgH_2, *i.e.* alloying, nanoscaling, nanoconfinement, adding additives. With these continuous efforts, some applaudable achievements are obtained, such as lower the operation temperature, enhance the kinetics, and extent the life-span. Despite of all the strategies above, there is still a long way to go to make MgH_2 commercial available, since no reports declares to fully meet the target of DOE.

The further researches on MgH_2/Mg may pay more attention on the following aspects: (1) Mechanism investigation. Fundamental information about the hydrogen diffusion and bonding process of MgH_2 should

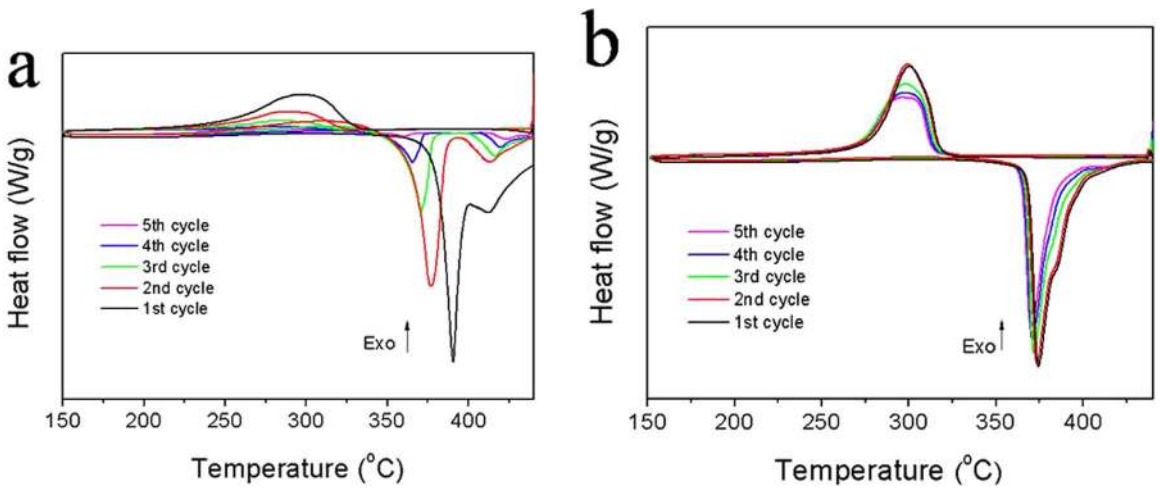

Fig. 11. Cycle life for (a) MgH_2, and (b) MgH_2-NiCo/rGO sample [105].

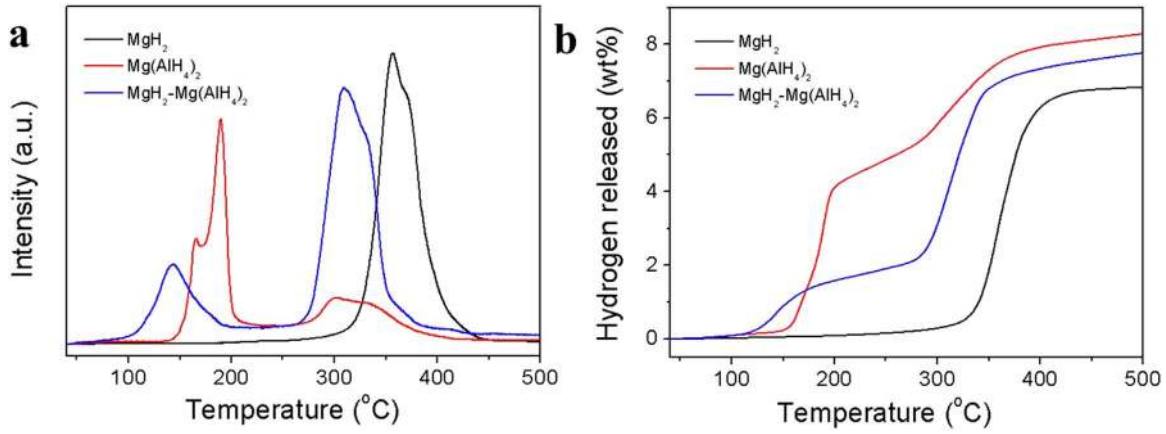

Fig. 12. (a) TPD, (b) dehydrogenation capacity curves for MgH_2-$Mg(AlH_4)_2$.

be investigated at atomic and molecular scales. The precise interaction between MgH_2 and additives are needed to explain. Advanced theoretical calculations may be helpful for understanding the hydrogenation/de-hydrogenation process of MgH_2. A basic understanding about MgH_2 is crucial for further researches.

(2) Exploring more efficient additives. Even same material can show different performance according to their morphology and structure, therefore, both the morphology and structure of additives can be optimized with the help of nanotechnology. And multifunctional materials needed to be synthesized, which should tailor the thermodynamics and kinetics of MgH_2 at the same time.

(3) Developing a novel approach to stabilize the MgH_2/Mg NPs. Reducing the particle size of MgH_2 into nanoscale is definitely a good way to tuning its hydrogen storage performance, but this high-energy structures can result serious aggregation and structure collapse during the dehydriding/hydriding. The usage of scaffolds, however, result in a significant capacity decrease. Finding a novel way to stabilize the MgH_2 NPs without scaffolds is important.

(4)Searching for more promising MgH_2-hydrid system. Researches about the MgH_2-hydrid system is still in its infant. Previous work had confirmed the advantages of different MgH_2-hydrid system, but none of them can meet all the requirements of DOE. More attention should be paid on this.

It is expected that with more effort focus on MgH_2/Mg system, significant breakthrough will gain to make it finally wide use in our real life.

Acknowledgment

This work was financially supported by the Research Fund for the Doctoral Program of Higher Education of China (20120031110001) and the Tianjin Science & Technology Project (10SYSYJC27600), the Priority Academic Program Development of Jiangsu Higher Education Institutions.

References

[1] S.J. Yang, H. Jung, T. Kim, C.R. Park, Prog. Nat. Sci. Mater. Int. 22 (2012) 631–638.
[2] E. Masika, R. Mokaya, Prog. Nat. Sci. Mater. Int. 23 (2013) 308–316.
[3] W. Lv, Y. Shi, W. Deng, J. Yuan, Y. Yan, Y. Wu, Prog. Nat. Sci. Mater. Int. 26 (2016) 177–181.
[4] H. Cao, Y. Zhang, J. Wang, Z. Xiong, G. Wu, P. Chen, Prog. Nat. Sci. Mater. Int. 22 (2012) 550–560.
[5] P. Jena, J. Phys. Chem. Lett. 2 (2011) 206–211.
[6] S.-i. Orimo, Y. Nakamori, J.R. Eliseo, A. Züttel, C.M. Jensen, Chem. Rev. 107 (2007) 4111–4132.
[7] P. Chen, Z. Xiong, G. Wu, Y. Liu, J. Hu, W. Luo, Scrip. Mater. 56 (2007) 817–822.
[8] ⟨http://energy.gov/eere/fuelcells/hydrogen-storage⟩
[9] R. von Helmolt, U. Eberle, J. Power Sources 165 (2007) 833–843.
[10] K.-F. Aguey-Zinsou, J.-R. Ares-Fernandez, Energy Environ. Sci. 3 (2010) 526–543.
[11] G. Xia, Y. Tan, X. Chen, D. Sun, Z. Guo, H. Liu, L. Ouyang, M. Zhu, X. Yu, Adv. Mater. 27 (2015) 5981–5988.
[12] N. Xing, Y. Wu, W. Han, S.-x. Zhou, Prog. Nat. Sci. Mater. Int. 20 (2010) 49–53.
[13] H. Reardon, N. Mazur, D.H. Gregory, Prog. Nat. Sci. Mater. Int. 23 (2013) 343–350.
[14] X. Xiao, C. Xu, J. Shao, L. Zhang, T. Qin, S. Li, H. Ge, Q. Wang, L. Chen, J. Mater. Chem. A 3 (2015) 5517–5524.
[15] Y. Zhang, B. Li, H. Ren, T. Yang, S. Guo, Y. Qi, D. Zhao, J. Mater. Sci. Technol. 32 (2016) 218–225.
[16] L. Zhang, J. Zhang, S. Han, Y. Li, S. Yang, J. Liu, Intermetallics 58 (2015) 65–70.
[17] J. Liu, S. Han, Y. Li, X. Zhao, S. Yang, Y. Zhao, Int. J. Hydrog. Energy 40 (2015) 1116–1127.
[18] J. Liu, S. Han, D. Han, Y. Li, S. Yang, L. Zhang, Y. Zhao, J. Power Sources 287 (2015) 237–246.
[19] W. Du, S. Cao, Y. Li, L. Zhang, Y. Zhao, S. Yang, S. Han, J. Electrochem. Soc. 162 (2015) A2180–A2187.
[20] L. Zhang, W. Du, S. Han, Y. Li, S. Yang, Y. Zhao, C. Wu, H. Mu, Electrochim. Acta 173 (2015) 200–208.
[21] J. Liu, S. Han, Y. Li, S. Yang, X. Chen, C. Wu, C. Ma, Electrochim. Acta 184 (2015) 257–263.
[22] T. Si, Y. Cao, Q. Zhang, D. Sun, L. Ouyang, M. Zhu, J. Mater. Chem. A 3 (2015) 8581–8589.
[23] Z. Cao, L. Ouyang, Y. Wu, H. Wang, J. Liu, F. Fang, D. Sun, Q. Zhang, M. Zhu, J. Alloy. Compd. 623 (2015) 354–358.
[24] M. Zhu, Y. Lu, L. Ouyang, H. Wang, Materials 6 (2013) 4654–4674.
[25] H. Wang, H.J. Lin, W.T. Cai, L.Z. Ouyang, M. Zhu, J. Alloy. Compd. 658 (2016) 280–300.
[26] J.F. Stampfer, C.E. Holley, J.F. Suttle, J. Am. Chem. Soc. 82 (1960) 3504–3508.
[27] M. Paskevicius, D.A. Sheppard, C.E. Buckley, J. Am. Chem. Soc. 132 (2010) 5077–5083.
[28] H.J. Lin, L.Z. Ouyang, H. Wang, D.Q. Zhao, W.H. Wang, D.L. Sun, M. Zhu, Int. J. Hydrog. Energy 37 (2012) 14329–14335.
[29] J.J. Reilly, R.H. Wiswall, Inorg. Chem. 7 (1968) 2254–2256.
[30] L.Z. Ouyang, F.X. Qin, M. Zhu, Scrip. Mater. 55 (2006) 1075–1078.
[31] V.M. Skripnyuk, E. Rabkin, Int. J. Hydrog. Energy 37 (2012) 10724–10732.
[32] J. Cui, H. Wang, J. Liu, L. Ouyang, Q. Zhang, D. Sun, X. Yao, M. Zhu, J. Mater. Chem. A 1 (2013) 5603–5611.
[33] H.C. Zhong, H. Wang, J.W. Liu, D.L. Sun, M. Zhu, Scr. Mater. 65 (2011) 285–287.
[34] T.Z. Si, J.B. Zhang, D.M. Liu, Q.A. Zhang, J. Alloy. Compd. 581 (2013) 246–249.
[35] J.J. Vajo, F. Mertens, C.C. Ahn, R.C. Bowman, B. Fultz, J. Phys. Chem. B 108 (2004) 13977–13983.
[36] D. Wu, L. Ouyang, C. Wu, H. Wang, J. Liu, L. Sun, M. Zhu, J. Alloy. Compd. 642 (2015) 180–184.
[37] M. Li, Y. Zhu, C. Yang, J. Zhang, W. Chen, L. Li, Int. J. Hydrog. Energy 40 (2015) 13949–13956.
[38] Y. Li, L. Zhang, Q. Zhang, F. Fang, D. Sun, K. Li, H. Wang, L. Ouyang, M. Zhu, J. Phys. Chem. C. 118 (2014) 23635–23644.
[39] X. Hou, R. Hu, T. Zhang, H. Kou, W. Song, J. Li, Int. J. Hydrog. Energy 39 (2014) 19672–19681.
[40] A.A.C. Asselli, J. Huot, Metals 4 (2014) 388–400.
[41] M. Retuerto, J.A. Alonso, R. Martinez, F. Jimenez-Villacorta, J. Sanchez-Benitez, M.T. Fernandez-Diaz, C.A. Garcia-Ramos, T. Ruskov, Int. J. Hydrog. Energy 40 (2015) 9306–9313.
[42] A.-L. Chaudhary, G. Li, M. Matsuo, S.-i. Orimo, S. Deledda, M.H. Sorby, B.C. Hauback, C. Pistidda, T. Klassen, M. Dornheim, Appl. Phys. Lett. 107 (2015).
[43] R.A. Varin, S. Li, C. Chiu, L. Guo, O. Morozova, T. Khomenko, Z. Wronski, J. Alloy. Compd. 404–406 (2005) 494–498.
[44] T. Liu, C. Qin, T. Zhang, Y. Cao, M. Zhu, X. Li, J. Mater. Chem. 22 (2012) 19831–19838.
[45] V. Bérubé, G. Radtke, M. Dresselhaus, G. Chen, Int. J. Energy Res. 31 (2007) 637–663.
[46] Y. Wang, Q. Zhang, Y. Wang, L. Jiao, H. Yuan, J. Alloy. Compd. 645 (Supplement

1) (2015) S509–S512.
[47] Y. Wang, L. Li, C. An, Y. Wang, C. Chen, L. Jiao, H. Yuan, Nanoscale 6 (2014) 6684–6691.
[48] Y. Wang, C. An, Y. Wang, Y. Huang, C. Chen, L. Jiao, H. Yuan, J. Mater. Chem. A 2 (2014) 16285–16291.
[49] W. Li, C. Li, H. Ma, J. Chen, J. Am. Chem. Soc. 129 (2007) 6710–6711.
[50] T. Spassov, U. Köster, J. Alloy. Compd. 287 (1999) 243–250.
[51] Y. Wu, W. Han, S.X. Zhou, M.V. Lototsky, J.K. Solberg, V.A. Yartys, J. Alloy. Compd. 466 (2008) 176–181.
[52] H.J. Lin, L.Z. Ouyang, H. Wang, J.W. Liu, M. Zhu, Int. J. Hydrog. Energy 37 (2012) 1145–1150.
[53] H. Gu, Y. Zhu, L. Li, Int. J. Hydrog. Energy 34 (2009) 2654–2660.
[54] W.Y. Li, C.S. Li, H. Ma, J. Chen, J. Am. Chem. Soc. 129 (2007) 6710 (-+).
[55] N.S. Norberg, T.S. Arthur, S.J. Fredrick, A.L. Prieto, J. Am. Chem. Soc. 133 (2011) 10679–10681.
[56] L.Z. Ouyang, S.Y. Ye, H.W. Dong, M. Zhu, Appl. Phys. Lett. 90 (2007) 021917.
[57] C. Zhu, S. Hosokai, I. Matsumoto, T. Akiyama, Cryst. Growth Des. 10 (2010) 5123–5128.
[58] C. Zhu, T. Akiyama, Cryst. Growth Des. 12 (2012) 4043–4052.
[59] T.K. Nielsen, K. Manickam, M. Hirscher, F. Besenbacher, T.R. Jensen, ACS Nano 3 (2009) 3521–3528.
[60] Z. Shu, F.G. Adam, L.V.A. Sky, L. Maribel, L. Ping, C.A. Channing, J.V. John, M.J. Craig, Nanotechnology 20 (2009) 204027.
[61] Z. Zhao-Karger, J. Hu, A. Roth, D. Wang, C. Kubel, W. Lohstroh, M. Fichtner, Chem. Commun. 46 (2010) 8353–8355.
[62] F.G. Adam, C.A. Channing, L.V.A. Sky, L. Ping, J.V. John, Nanotechnology 20 (2009) 204005.
[63] P.Ed Jongh, R.W.P. Wagemans, T.M. Eggenhuisen, B.S. Dauvillier, P.B. Radstake, J.D. Meeldijk, J.W. Geus, K.Pd Jong, Chem. Mater. 19 (2007) 6052–6057.
[64] Y.S. Au, M.K. Obbink, S. Srinivasan, P.C.M.M. Magusin, K.P. de Jong, P.E. de Jongh, Adv. Funct. Mater. 24 (2014) 3604–3611.
[65] M. Konarova, A. Tanksale, J. Norberto Beltramini, G. Qing Lu, Nano Energy 2 (2013) 98–104.
[66] H. Wang, S.F. Zhang, J.W. Liu, L.Z. Ouyang, M. Zhu, Mater. Chem. Phys. 136 (2012) 146–150.
[67] Y.S. Au, M.K. Obbink, S. Srinivasan, P.C.M.M. Magusin, K.P. de Jong, P.E. de Jongh, Adv. Funct. Mater. 24 (2014) 3604–3611.
[68] J.L. Bobet, E. Akiba, Y. Nakamura, B. Darriet, Int. J. Hydrog. Energy 25 (2000) 987–996.
[69] A. Denis, E. Sellier, C. Aymonier, J.L. Bobet, J. Alloy. Compd. 476 (2009) 152–159.
[70] G. Liang, J. Huot, S. Boily, A. Van Neste, R. Schulz, J. Alloy. Compd. 292 (1999) 247–252.
[71] J.L. Bobet, B. Chevalier, M.Y. Song, B. Darriet, J. Etourneau, Mater. Manuf. Process. 17 (2002) 351–361.
[72] J. Zou, X. Zeng, Y. Ying, X. Chen, H. Guo, S. Zhou, W. Ding, Int. J. Hydrog. Energy 38 (2013) 2337–2346.
[73] J.F. Pelletier, J. Huot, M. Sutton, R. Schulz, A.R. Sandy, L.B. Lurio, S.G.J. Mochrie, Phys. Rev. B 63 (2001).
[74] A. Zaluska, L. Zaluski, J.O. Ström–Olsen, J. Alloy. Compd. 288 (1999) 217–225.
[75] X. Xu, C. Song, Appl. Catal. A: Gen. 300 (2006) 130–138.
[76] H. Gasan, O.N. Celik, N. Aydinbeyli, Y.M. Yaman, Int. J. Hydrog. Energy 37 (2012) 1912–1918.
[77] W. Oelerich, T. Klassen, R. Bormann, J. Alloy. Compd. 322 (2001) L5–L9.
[78] M. Song, J.-L. Bobet, B. Darriet, J. Alloy. Compd. 340 (2002) 256–262.
[79] M. Polanski, J. Bystrzycki, J. Alloy. Compd. 486 (2009) 697–701.
[80] G. Barkhordarian, T. Klassen, R. Bormann, J. Alloy. Compd. 407 (2006) 249–255.
[81] C. An, Y. Wang, Y. Huang, Y. Xu, L. Jiao, H. Yuan, Nano Energy 10 (2014) 125–134.
[82] M. Polanski, J. Bystrzycki, J. Alloy. Compd. 486 (2009) 697–701.
[83] S. Milosevic, Z. Raskovic-Lovre, S. Kurko, R. Vujasin, N. Cvjeticanin, L. Matovic, J.G. Novakovic, Ceram. Int. 39 (2013) 51–56.
[84] E. Ivanov, I. Konstanchuk, B. Bokhonov, V. Boldyrev, J. Alloy. Compd. 359 (2003) 320–325.
[85] S.-A. Jin, J.-H. Shim, Y.W. Cho, K.-W. Yi, J. Power Sources 172 (2007) 859–862.
[86] A. Ranjbar, Z.P. Guo, X.B. Yu, D. Attard, A. Calka, H.K. Liu, Int. J. Hydrog. Energy 34 (2009) 7263–7268.
[87] M.P. Pitt, M. Paskevicius, C.J. Webb, D.A. Sheppard, C.E. Buckley, E.M. Gray, Int. J. Hydrog. Energy 37 (2012) 4227–4237.
[88] W. Oelerich, T. Klassen, R. Bormann, J. Alloy. Compd. 315 (2001) 237–242.
[89] H. Shin, M. Choi, H. Kim, Phys. Chem. Chem. Phys. 18 (2016) 7035–7041.
[90] Y. Chen, Y. Liu, J. Mater. Chem. A 2 (2014) 9193–9199.
[91] M.S.L. Hudson, K. Takahashi, A. Ramesh, S. Awasthi, A.K. Ghosh, P. Ravindran, O.N. Srivastava, Catal. Sci. Tech. 6 (2016) 261–268.
[92] G. Barkhordarian, T. Klassen, R. Bormann, J. Alloy. Compd. 364 (2004) 242–246.
[93] Y. Kojima, Y. Kawai, T. Haga, J. Alloy. Compd. 424 (2006) 294–298.
[94] S.T. Sabitu, G. Gallo, A.J. Goudy, J. Alloy. Compd. 499 (2010) 35–38.
[95] B.S. Amirkhiz, B. Zahiri, P. Kalisvaart, D. Mitlin, Int. J. Hydrog. Energy 36 (2011) 6711–6722.
[96] G. Liu, Y.J. Wang, C. Xu, F. Qiu, C. An, L. Li, L.F. Jiao, H.T. Yuan, Nanoscale 5 (2013) 1074–1081.
[97] M.A. Lillo-Ródenas, Z.X. Guo, K.F. Aguey-Zinsou, D. Cazorla-Amorós, A. Linares-Solano, Carbon 46 (2008) 126–137.
[98] S. Nohara, H. Inoue, Y. Fukumoto, C. Iwakura, J. Alloy. Compd. 252 (1997) L16–L18.
[99] S. Bouaricha, J.P. Dodelet, D. Guay, J. Huot, R. Schulz, J. Alloy. Compd. 325 (2001) 245–251.
[100] G. Liu, Y. Wang, L. Jiao, H. Yuan, Int. J. Hydrog. Energy 39 (2014) 3822–3829.
[101] W. Su, Y. Zhu, J. Zhang, Y. Liu, Y. Yang, Q. Mao, L. Li, J. Alloy. Compd. 669 (2016) 8–18.
[102] C. An, G. Liu, L. Li, Y. Wang, C. Chen, Y. Wang, L. Jiao, H. Yuan, Nanoscale 6 (2014) 3223–3230.
[103] Y. Wang, G. Liu, C. An, L. Li, F. Qiu, Y. Wang, L. Jiao, H. Yuan, Chem. Asian J. 9 (2014) 2576–2583.
[104] G. Liu, Y. Wang, F. Qiu, L. Li, L. Jiao, H. Yuan, J. Mater. Chem. 22 (2012) 22542–22549.
[105] Y. Wang, G. Liu, C. An, L. Li, F. Qiu, Y. Wang, L. Jiao, H. Yuan, Chem. Asian J. 9 (2014) 2576–2583.
[106] N.S. Mustafa, M. Ismail, Int. J. Hydrog. Energy 39 (2014) 7834–7841.
[107] H. Liu, X. Wang, Y. Liu, Z. Dong, H. Ge, S. Li, M. Yan, J. Phys. Chem. C 118 (2014) 37–45.
[108] S.R. Johnson, P.A. Anderson, P.P. Edwards, I. Gameson, J.W. Prendergast, M. Al-Mamouri, D. Book, I.R. Harris, J.D. Speight, A. Walton, Chem. Commun. (2005) 2823–2825.
[109] T. Czujko, R.A. Varin, Z. Wronski, Z. Zaranski, T. Durejko, J. Alloy. Compd. 427 (2007) 291–299.
[110] P. Plerdsranoy, R. Utke, J. Phys. Chem. Solids 90 (2016) 80–86.
[111] P. Plerdsranoy, S. Meethom, R. Utke, J. Phys. Chem. Solids 87 (2015) 16–22.